

Supporting Online Material Regarding New Impact Sites on Mars that Formed Between May 1999 and March 2006

Michael C. Malin, Kenneth S. Edgett, Liliya V. Posiolova, Shawn M. McColley, and Eldar Z. Noe Dobrea, Malin Space Science Systems, Inc., San Diego, California, USA

Introduction

This document constitutes Supporting Online Material that accompanies a paper published in *Science* by M. C. Malin, *et al.*, regarding impact craters formed on the martian surface between May 1999 and March 2006. A more detailed treatment—including unprocessed data, pictures of each impact site, and before and after impact images—are captured in a catalog provided by the Malin Space Science Systems web site: <http://www.msسس.com/crater2006catalog/>. However, this is not an archival site and might not persist for decades to come. Thus, the reader is encouraged to seek the raw Mars Global Surveyor (MGS) Mars Orbiter Camera (MOC) and other image data described here (particularly in Tables S1 and S2) archived with the National Aeronautics and Space Administration Planetary Data System (NASA PDS): <http://pds.jpl.nasa.gov/>.

Background

This study grew out of a single observation made in January 2006. As illustrated in Figure 1a of the *Science* paper, a dark spot was noticed in a MOC red wide angle camera (~230 m/pixel) context image acquired on 6 January 2006. This spot was not present in previous red wide angle images, such as MOC E05-00855 from June 2001. We recalled that this spot resembled that which surrounds a small (~25 m diameter), fresh impact crater identified previously near the summit of Ulysses Patera (Figure S1). In the Ulysses Patera case, the dark spot in red wide angle images is the product of ejecta deposition and—more importantly—the disturbance of dust radial to site at the time the impact occurred. The Ulysses Patera ~25 m diameter crater was not present in Viking orbiter images, and thus was deduced to have formed in the 1980s (or later, depending upon the rate at which dust covers and obscures the feature over time).

The new spot (*Science* paper, Figure 1a), owing to its similarity to the spot at Ulysses Patera (Figure S1), was hypothesized to be a fresh impact crater. In this case, it had to be one that formed after 12 November 2004, because it was absent in a Mars Odyssey Thermal Emission System (THEMIS) visible subsystem (VIS) image, V1294012, acquired on that date.

At the first available opportunity, on 20 February 2006, the dark spot in the *Science* paper Figure 1a was targeted for acquisition of a MGS MOC image using the Roll Only Targeted Observation (ROTO) technique (S1). Without employment of the ROTO technique to slew the spacecraft such that the instrument deck pointed at the desired target, we would have had to wait anywhere from a few months to several years for an orbital ground track to pass the MOC over the site. When the 20 February 2006 image was finally acquired and returned to Earth, we found that, indeed, the dark spot was caused by an impact (*Science* paper, Figure 1b).

Even before we confirmed that the dark spot was the site of a recent impact, we realized that other new dark spots might also occur on Mars, and that some of these—whether the first one was a crater or not—might mark the locations of recent impacts. Our experience from MOC suggested that we'd have the most success looking for fresh impact sites by seeking new dark spots that occur in the dustiest regions of the planet. Thermal inertia maps derived from Viking orbiter Infrared Thermal Mapper (IRTM) observations, more than two decades ago, pinpointed the Tharsis, Amazonis, and Arabia regions of Mars as being mantled by dust (S2), and MOC high resolution images confirmed this view (S3).

The reason we considered that dusty regions would provide the most chances for success comes from two issues:

- (1) The majority of very recent impact craters are likely to be small (< 200 meters in diameter). MOC consists of 3 cameras, a narrow angle instrument that can obtain images of 0.5 – 12.0 m/pixel spatial resolution over 3 km-wide swaths, and two wide angle cameras (1 red- and 1 blue-filtered) that can cover terrain from limb to limb, achieving their highest spatial resolution near nadir at around 240 m/pixel (S4, S5). The narrow angle camera has only covered about 5.2% of the martian surface since it began operation in September 1997. But the wide angle cameras have covered the entire planet. In May–June 1999, we conducted the MOC Geodesy Campaign (S6) and mapped the entire surface with the red wide angle camera at ~230 m/pixel (north of the location of the southern terminator during that month; later campaigns filled in the south high latitudes and Hellas Planitia, which was obscured by dust in May 1999). Thus, we needed to be able to search for new craters, which will typically be < 100 m/pixel in size, using a camera that had covered the dusty regions during the May–June 1999 period at 230 m/pixel. The dark spots seen in the red wide angle images presented the examples of how this would be done—you re-image these regions in 2006 with the same red wide angle camera and look for new dark spots. Such spots would be candidate fresh impact sites.
- (2) In the dust-mantled Tharsis region, we knew from MOC results of two impact sites for which the zone of disrupted surface material far exceeded the diameter of the impact crater. These may be the result of atmospheric interaction with the dust during the impact event. The first such example is in Figure S1, but a better example is seen in Figure S2. In this case, a 130 m diameter crater is located among rays which radiate away from the impact site (asymmetrically, perhaps owing to the entry geometry of the impactor) to distances of in excess of 6 km. A small impact in a dusty region, this experience suggests, will disrupt the surface to distances sufficient to darken several pixels in a 230 m/pixel red wide angle camera image.

Data Collection and Analysis

The new impacts we have documented all occurred between the MOC Geodesy Campaign in May–June 1999 and our new red wide angle camera survey in January–March 2006. There are two sets of methods discussed in this section; the first describes how we found the new impact sites, the second describes how we further constrained the time at which each impact occurred. In several cases, we constrained the date of the

impact to a period of ≤ 3 months, and in all cases we have constrained the dates to periods less than May 1999 – March 2006.

Throughout this document, the location of features on Mars are given using the traditional areographic latitude and west-positive longitude coordinate system; a system dating back more than a century that has served the MOC team well enough to be able to routinely rotate the MGS spacecraft off nadir and hit targets with a 3 km wide field of view to within 100 meters.

Finding The New Impact Sites

The first step in finding the new impact sites was to acquire in 2006 a suite of MOC red wide angle camera views at ~ 230 m/pixel that repeat much of Amazonis, Tharsis, and Arabia. These areas were previously covered by the same camera at the same spatial scale during the 1999 Geodesy Campaign.

The next step was to compare the 2006 and 1999 MOC red wide angle images, to identify new dark spots. This step began with the acquisition of the first MOC red wide angle images and continued in parallel with the acquisition of new images that cover these regions.

The third step was to enter these dark spots into a database of targets that have been identified for the MOC narrow angle camera. Once each week, the locations of features in the database were compared with the latest predicted orbit ground tracks for a subsequent week, and opportunities to perform a ROTO maneuver (slew the spacecraft up to 29.9° off nadir (*S1*)) were identified and commanded. These images were always commanded to have full spatial resolution, ~ 1.5 m/pixel.

Following acquisition of the MOC narrow angle image of a candidate impact site, the image was examined to determine whether the dark spot identified in MOC red wide angle images was indeed the product of an impact or the result of some other process (eolian, mass movement, etc.).

In a few cases, we desired a higher resolution view of the site. We entered those cases into the database as candidates for imaging using the cPROTO (compensated Pitch and Roll Targeted Observations) technique (*S7*). Images acquired in this manner have a spatial resolution of about 0.5 m/pixel in the down-track dimension, 1.5 m/pixel in the cross-track dimension. When opportunities presented themselves to acquire images of the impact sites with this technique, we made the attempt. Not all cPROTO images hit their targets, however, and in some cases it takes 3 to 6 attempts before the target is hit (*S7*).

Constraining the Age of New Impact Sites

Once a new impact site was confirmed by acquiring a MOC narrow angle camera image using the ROTO technique, we then attempted to constrain the time at which the impact occurred. Each one of these impacts is already constrained to having occurred between the May–June 1999 Geodesy Campaign, and the January–March 2006 periods when we acquired new red wide angle camera views. A key motivator for determining the more

narrow range of time in which the impact occurred was to determine whether craters that occur in the same region formed at the same or different times—that is, whether they represent singular impact events, or are the product of secondary cratering from some larger, primary impact.

By examining all of the images acquired by orbiting spacecraft during the May 1999 – March 2006 period, we found that we could constrain the timing of each impact to a narrower range. The data examined were:

- (1) All MGS MOC wide angle images of better than 250 m/pixel spatial resolution and all narrow angle images of the impact sites, acquired through July 2006.
- (2) All Mars Odyssey THEMIS (S8) day and night thermal infrared (band 9) images, each of ~100 m/pixel spatial resolution, plus all THEMIS VIS (visible subsystem) images, for each impact site, acquired through July 2006.
- (3) All Mars Express High Resolution Stereo Camera (HRSC; S9) images of the impact sites, acquired through June 2005 (*i.e.*, data that were available in the publicly-released data archives as of July 2006).

We found that night-time THEMIS infrared images in these regions usually had insufficient signal-to-noise quality to be able to distinguish the impact sites, but we did check them as well as the daytime thermal infrared data.

Results

With the red wide angle camera survey conducted in January – March 2006, we covered 21,506,629 km², and identified 39 candidate dark spots. The areas covered by the red wide angle camera are shown in Figure S3. These were targeted by MGS MOC during February – April 2006 using the ROTO technique. Some sites were re-targeted at higher resolution using the cPROTO approach. Of the 39 candidates, 20 were found to be new impact craters and 19 were not. Table S1 summarizes these observations.

Table S2 lists the images and dates those images were acquired which constrain the time that each of the 20 new impacts occurred. We found that some craters could be pinned down to having formed within very short periods of less than a few months—one was constrained to a 40 day period, largely covering January 2006, the time when the study was begun. By determining that the craters formed during different periods of the May 1999 – March 2006 range, we were also able to confirm that these impacts were primary, not secondary events. Figure S4 shows a particularly good example, in which two dark spots formed with a few hundred kilometers of each other, but in different years.

The number of craters identified from this study should be considered a lower limit. Atmospheric haze and deposition of dust, over time, might obscure some fresh craters. We believe that dust obscuration was not a major factor, however, because (a) the crater and dark rays in Figure S2, above, have remained visible as a dark spot on the martian surface since at least 1972; (b) the crater in Figure S1, above, has remained dark since some time before 1999, perhaps since the 1980s; and (c) we found early in the MGS

mission via examination of MOC images that dust deposition is non-uniform over the planet (*S10*); this non-uniform pattern was also observed following the 2001 global dust storm events (*S11*).

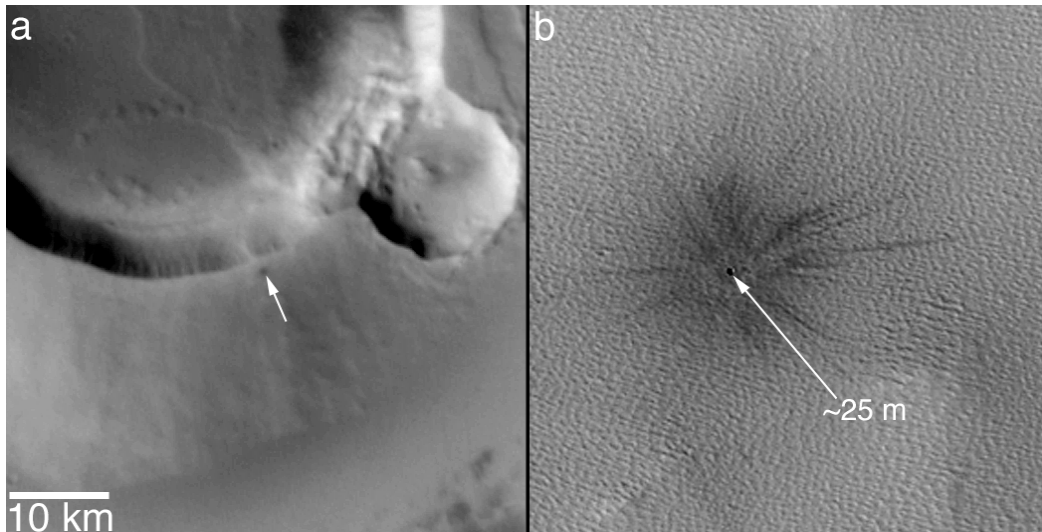


Figure S1. Impact site on Ulysses Patera, known since October 1999. **(a)** Dark spot (arrow) seen in MOC red wide angle context frame acquired at the same time as the narrow angle camera view to the right. This is a sub-frame of MOC M08-01171. **(b)** Small, ~25 m diameter crater and dark, rayed ejecta pattern in a sub-frame of MOC M08-01170. North is up.

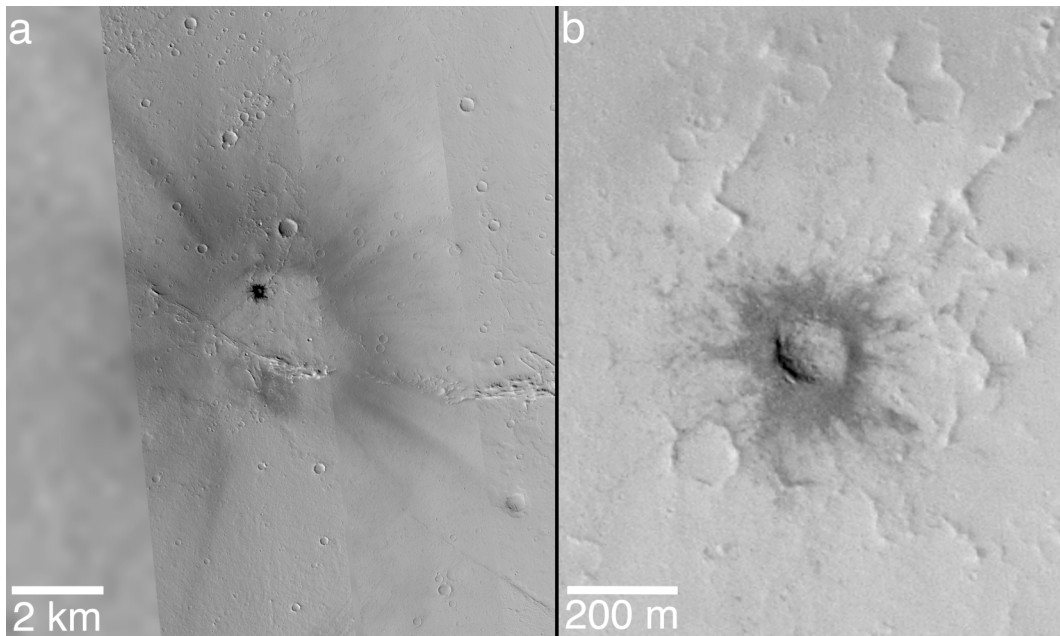


Figure S2. **(a)** Small, dark, fresh impact site in Tharsis that has been present in the region since some time before the Mariner 9 observed a dark spot at this location in 1972 in image DAS 7039378. This is a composite of MOC images E05-01904, M21-00272, and M08-03697, and Viking 1 image 516A55. Note the rays, indicating a zone in which surface dust was disrupted many kilometers from the site. **(b)** Close-up view of the crater. North is up.

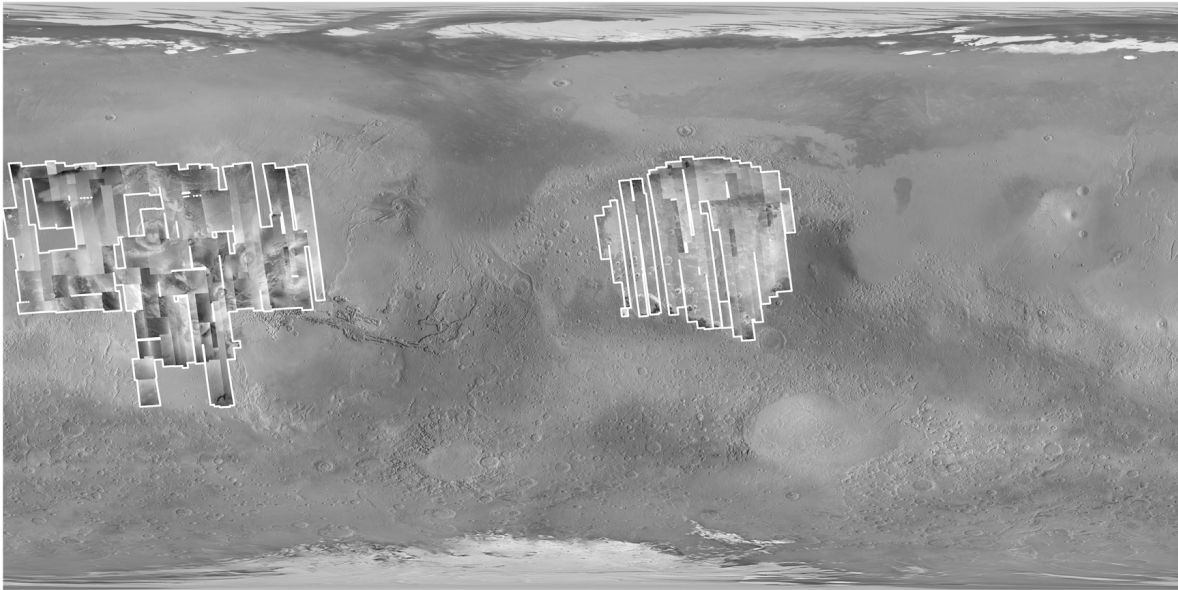


Figure S3. Simple cylindrical map of Mars showing the areas covered for this study by MGS MOC red wide angle camera images during January – March 2006. These data cover much of the dust-covered regions of Amazonis, Tharsis, and Arabia. The area examined is 21,506,629 km².

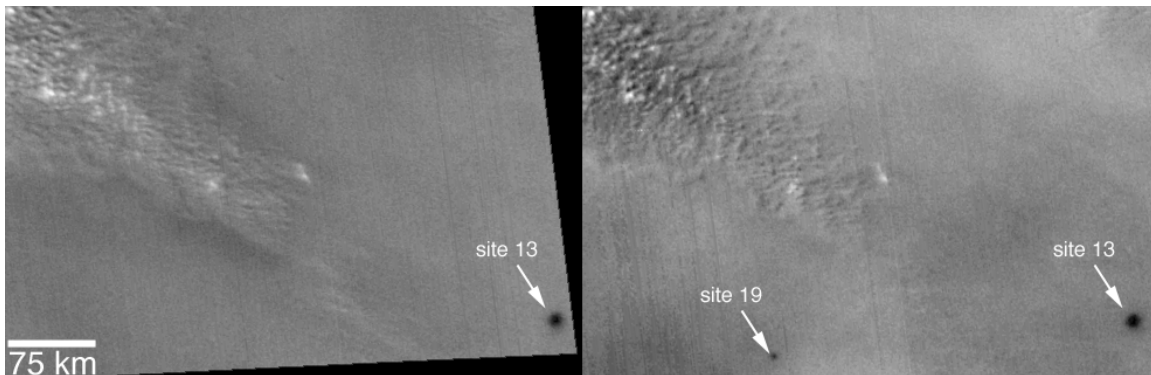


Figure S4. Two fresh impact sites near each other in Tharsis, south of Olympus Mons, demonstrate that the craters identified by this study are not secondary impacts related to some other, larger event. The picture on the left shows a dark spot at impact site 13, which has been constrained by orbiter images to have formed between 2 June 1999 and 20 August 2003. On the right, a new impact occurred at site 19 between 22 January and 22 April 2004. The timing of these impacts does not overlap, the first formed before 20 August 2003, the second after 22 January 2004. Both images are simple cylindrical projections (north is up) of sub-frames of MOC red wide angle images R13-03428 (left) and S17-01973 (right).

Table S1: Results of MOC Survey for New Impact Craters in the Study Regions

Site	Latitude	Longitude	MOLA Elevation (km)	MOC NA	Image first spotted in (sample, line)	Result and, if Crater, then Diameter	
1	14.0°N	151.5°W	-3.63	S15-02128	S14-00672 (s=131, l=295)	Multiple craters	19.1 (7 @ 10 m) ± 1.7 m
2	25.8°N	308.0°W	-0.25	S15-02322	S14-03311 (s=347, l=6367)	New impact site	16 ± 1.7 m
3	0.8°S	160.0°W	-1.38	S15-02488	S14-02683 (s=443, l=957)	New impact site	17 ± 3.0 m
4	23.3°N	307.2°W	0.38	S15-02522	S14-03311 (s=421, l=5738)	New impact site	15.6 ± 1.7 m
5	20.6°N	356.8°W	-2.00	S15-02724	S15-00478 (s=337, l=2280)	New impact site	22.6 ± 3.0 m
6	20.0°N	152.7°W	-3.88	S16-00097	S15-01354 (s=542, l=3246)	New impact site	12.6 ± 3.0 m
7	0.0°	133.2°W	1.00	S16-02226	S15-01463 (s=894, l=1573)	Multiple craters	26.6 (22.4, 15.4, 12.6, 12.6) ± 3.0 m
8	2.5°N	136.0°W	0.25	S16-00855	S15-01463 (s=330, l=2240)	Multiple craters	36.7 (29.6, 21.6, 19.6, 18.2) ± 3.0 m
9	11.5°N	156.6°W	-3.63	S16-01063	S15-00190 (s=1540, l=1295)	New impact site	11.2 ± 3.0 m
10	29.3°N	333.2°W	-1.75	S16-01105	S14-02741 (s=170, l=3223)	New impact site	11.2 ± 3.0 m
11	27.3°N	91.8°W	2.25	S16-01140	R15-01052 (s=218, l=346)	New impact site	19.8 ± 3.0 m
12	22.2°N	345.5°W	-1.50	S16-01199	S15-00351 (s=73, l=6791)	New impact site	24 ± 3.0 m
13	5.5°N	135.7°W	0.88	S18-00653	S15-01463 (s=476, l=2958)	New impact site	28.2 ± 3.0 m
14	26.4°N	336.5°W	-1.50	S16-01674	S14-03323 (s=364, l=7284)	New impact site	22.6 ± 1.7 m
15	1.7°N	160.7°W	-1.88	S17-00774	S16-00224 (s=765, l=505)	New impact site	14.0 ± 3.0 m
16	13.9°N	84.4°W	0.13	S17-00998	S15-02768 (s=383, l=3665)	Multiple craters	12.6 (12.4, 4.2) ± 1.7 m
17	25.7°S	136.2°W	2.00	S17-01187	S15-02021 (s=500, l=1915)	New impact site	148 ± 3 m
18	28.7°N	334.9°W	-1.75	S17-01561	S15-02721 (s=209, l=3815)	Multiple craters	12.6 (12.0, 6.0) ± 3.0 m
19	5.4°N	136.8°W	0.63	S17-01972	S15-01463 (s=247, l=2953)	Multiple craters	10.2 (10.0, 4.0) ± 3.0 m
20	7.0°N	112.2°W	3.38	S18-00492	S15-02778 (s=165, l=2861)	Multiple craters	20.5 (16.8, 11.2, 11.5, 6, 6, 6) ± 3.0 m
a	17.4°N	312.1°W		S16-01371	S15-01292 (s=330, l=6161)	New group of dark slope streaks	
b	11.7°S	111.7°W		S16-01146	S15-00274 (s=188, l=1876)	No dark spot	
c	37.4°N	145.0°W		S16-01154	S15-01047 (s=1178, l=1614)	Dark windblown albedo feature	
d	3.8°N	304.0°W		S16-01097	S14-03311 (s=567, l=970)	No dark spot	
e	1.7°N	129.8°W		S16-00376	S14-02929 (s=193, l=472)	Dark windblown albedo feature	
f	32.7°N	116.0°W		S15-02952	S15-00036 (s=1837, l=195)	Dark spot was shadow of large dust devil	
g	31.6°N	93.8°W		S16-01701	S15-01556 (s=348, l=6241)	Dark windblown albedo feature	
h	23.0°N	96.4°W		S16-02573	S15-01339 (s=284, l=4394)	Dark wind-streaked surface	
i	1.5°N	91.4°W		S17-00062	S14-02924 (s=1476, l=1247)	Dark wind-streaked surface	
j	5.9°N	150.9°W		S17-00083	S14-02932 (s=1716, l=1253)	Dark wind-streaked surface	
k	27.7°N	92.2°W		S17-00250	S15-01556 (s=539, l=5244)	Dark wind-streaked surface	
l	36.8°N	149.0°W		S17-00275	S15-01047 (s=483, l=1515)	Rough surface	
m	31.6°S	134.1°W		S17-00439	S15-02021 (s=754, l=451)	Crater not new, visible in MOC M03-00225	
n	29.1°N	113.7°W		S17-00605	S15-02017 (s=929, l=2297)	Dark wind-streaked surface	
o	30.4°S	136.4°W		S17-01009	S15-02021 (s=336, l=796)	Crater not new, in Viking and early MOC data	
p	26.8°S	133.5°W		S17-01366	S15-02021 (s=1038, l=1599)	Crater not new, in M01-00703, Viking 457a20	
q	26.9°S	137.2°W		S17-02403	S15-02021 (s=272, l=1671)	Crater not new, in Viking 457a11, 457a13	
r	25.3°S	135.4°W		S18-00047	S15-02021 (s=702, l=1991)	Crater not new, see spot in MOC M01-04652	
s	2.2°N	129.6°W		S18-00961	S14-02929 (s=225, l=582)	Dark windblown albedo feature	

Table S2: Images and Dates Constraining Time of Impact For 20 New Craters

Impact Site	Last Image Before Impact	First Image After Impact	Dates Constraining Time of Impact	Other Important Post-Impact Images
1	THEMIS V12924012	MOC S14-00672	12 November 2004 – 6 January 2006	MOC S15-02128, MOC S16-01426
2	THEMIS V17834021	MOC S14-03311	21 December 2005 – 31 January 2006	MOC S15-02322, MOC S17-01393
3	THEMIS I03951001	THEMIS I11228001	4 November 2002 – 25 June 2004	MOC S15-02488
4	MOC E01-00237	MOC S07-01349	4 February 2001 – 13 June 2005	MOC S15-02522, MOC S16-01666
5	THEMIS I02409005	MOC R05-00630	30 June 2002 – 7 May 2003	MOC S15-02724, THEMIS I08014019
6	THEMIS I17267007	MOC S15-01354	5 November 2005 – 13 February 2006	MOC S16-00097
7	THEMIS I10652014	MOC S15-01463	9 May 2004 – 17 February 2006	MOC S16-00667, MOC S16-02226
8	THEMIS I10103010	THEMIS I10727005	25 March 2004 – 15 May 2004	MOC S16-00855, THEMIS V15020008
9	MOC E13-00919	THEMIS I07645020	11 February 2002 – 4 September 2003	MOC S16-01063, THEMIS V09954010 and V14871023
10	MOC R05-00427	MOC S05-01885	5 May 2003 – 29 April 2005	MOC S16-01105
11	MOC R04-01354	THEMIS I09540014	18 April 2003 – 7 February 2004	MOC S16-01140, HRSC H1052_0000_ND3
12	MOC E03-00127	MOC R12-01350	2 April 2001 – 11 December 2003	MOC S16-01199
13	MOC M01-05675	THEMIS I07457015	2 June 1999 – 20 August 2003	MOC S16-01331 and S18-00653, THEMIS V13797015
14	MOC R12-00786	THEMIS I17523014	8 December 2003 – 26 November 2005	MOC S16-01674, S17-00795, S17-02191, S18-01407, and S20-01581
15	THEMIS I07720022	THEMIS I09405011	11 September 2003 – 27 January 2004	MOC S17-00774, THEMIS V13698008 and V17080020
16	THEMIS I09652013	MOC S15-02768	17 February 2004 – 26 February 2006	MOC S17-00998, MOC S18-01821
17	MOC E02-02262	THEMIS I04755006	25 March 2001 – 9 January 2003	MOC S17-01187
18	HRSC H1483_0000_ND3	MOC S15-02721	14 March 2005 – 26 February 2006	MOC S17-01561
19	MOC R13-03428	THEMIS I10440047	22 January 2004 – 22 April 2004	MOC S17-01972, THEMIS V11975013
20	THEMIS I16679016	MOC S15-02778	17 September 2005 – 26 February 2006	MOC S18-00492

References

- S1. M. Malin et al., *Lunar Planet. Sci.* **XXXV**, 1189 (2004).
- S2. P. R. Christensen, *J. Geophys. Res.* **91**, 3533–3545 (1986).
- S3. M. C. Malin, K. S. Edgett, *J. Geophys. Res.* **106**, 23,429, 10.1029/2000JE001455 (2001).
- S4. M. C. Malin et al., *Int. J. Imag. Syst. Tech.* **3**, 76 (1991).
- S5. M. C. Malin et al., *J. Geophys. Res.* **97**, 7699 (1992).
- S6. M. A. Caplinger, M. C. Malin, *J. Geophys. Res.* **106**, 23,595, 10.1029/2000JE001341 (2001).
- S7. M. C. Malin, K. S. Edgett, *Lunar Planet. Sci.* **XXXVI**, 1172 (2005).
- S8. P. R. Christensen et al., *Space Sci. Rev.* **110**, 85, 10.1023/B:SPAC.0000021008.16305.94 (2004).
- S9. G. Neukum, R. Jaumann, in *Mars Express: The Scientific Payload*, A. Wilson, Ed. (European Space Agency SP-1240, Noordwijk, Netherlands, 2004), pp. 17–35.
- S10. K. S. Edgett, M. C. Malin, *J. Geophys. Res.* **105**, 1623, 10.1029/1999JE001152 (2000).
- S11. B. A. Cantor, *Icarus*, 10.1016/j.icarus.2006.08.019 (2006).